

MINX Document 5

Measuring Aerosol Height and Motion with MINX



David Nelson

**Raytheon Company, Jet Propulsion Laboratory,
California Institute of Technology**

January, 2013



Contents

- **Parallax, disparity and image matching**
- **Height/wind retrieval algorithm**
- **MINX height retrieval comparisons**

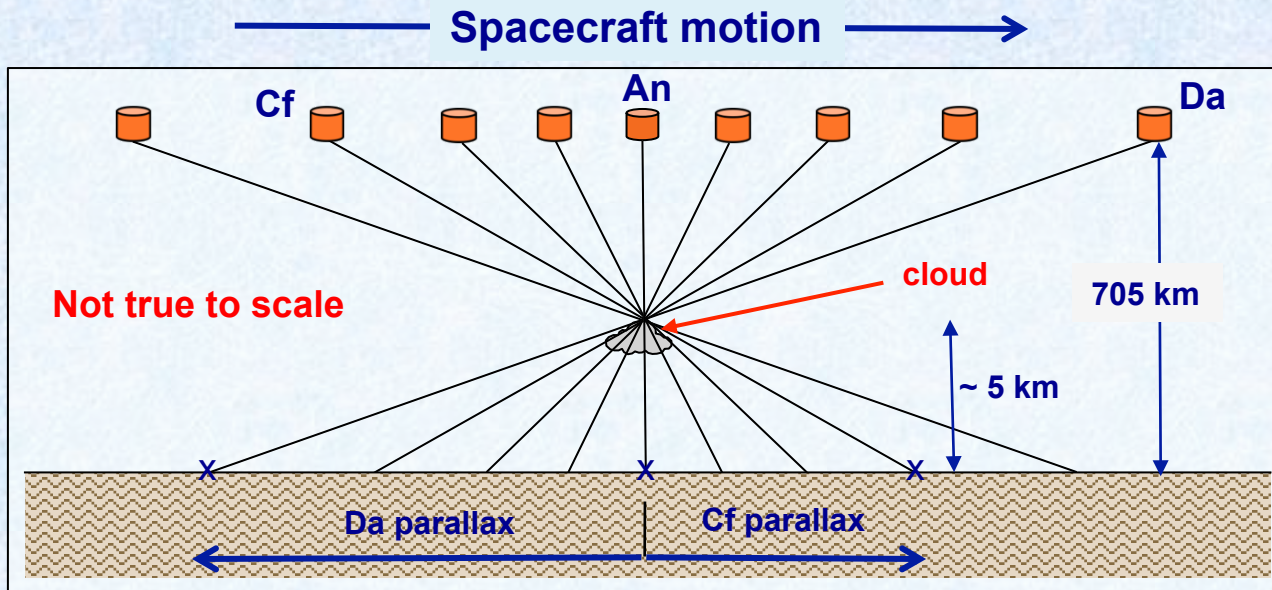
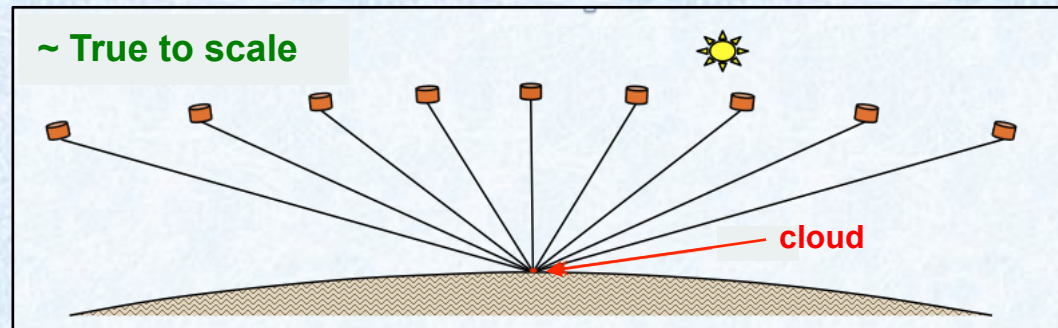
Contents

- **Parallax, disparity and image matching**
- **Height/wind retrieval algorithm**
- **MINX height retrieval comparisons**

Parallax

Parallax is a difference in the apparent position of an object viewed along different lines of sight. Nearby objects have larger parallax than more distant objects, so parallax can be used to determine distance.

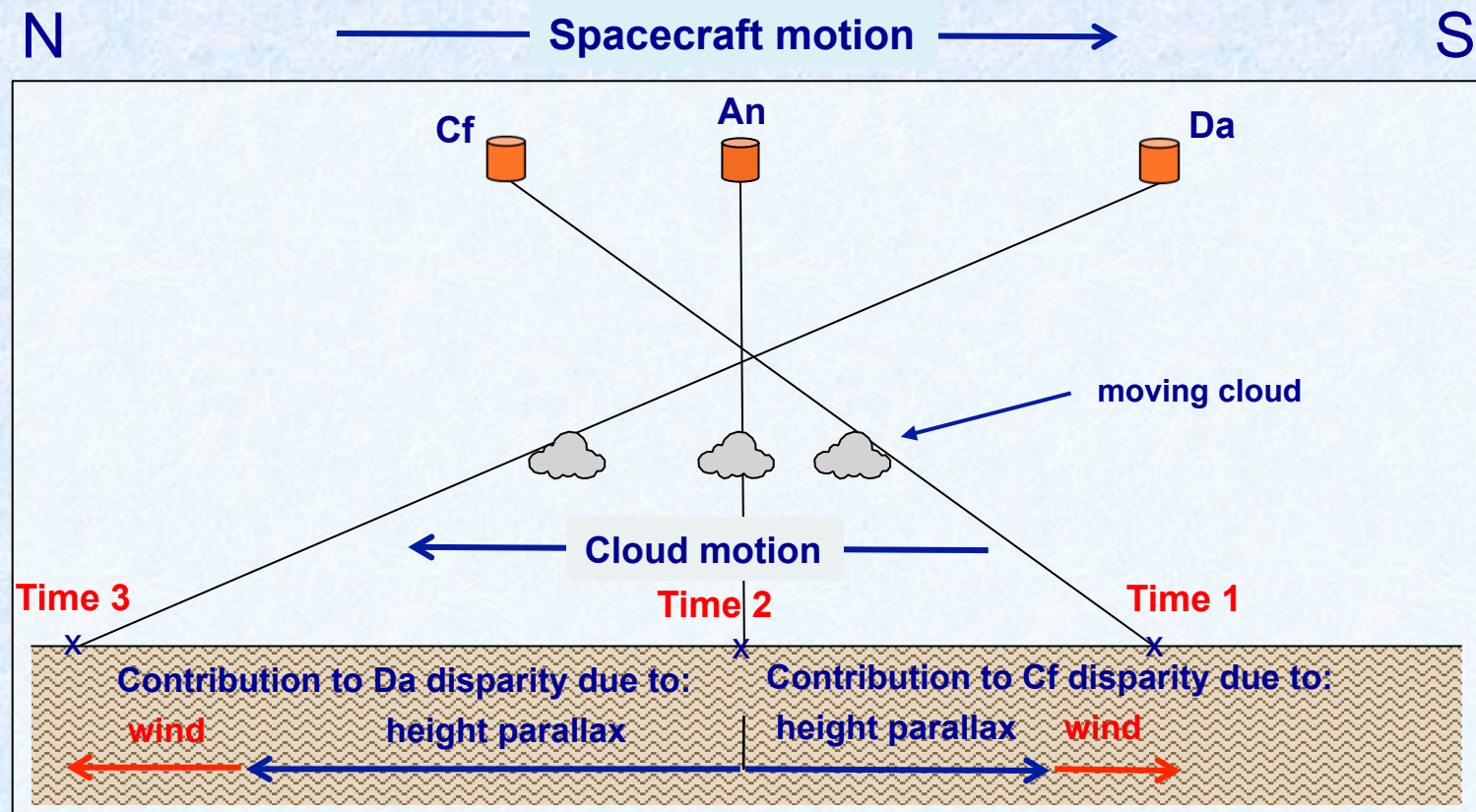
MISR geometry when all cameras view a stationary cloud



Da and Cf camera parallax relative to An camera

Disparity - 1

Disparity is closely related to parallax. It is the measure of total offset in the apparent position of an object viewed along different lines of sight due to actual **movement of the object** in addition to height parallax. In MINX, the direction of cloud (or plume) motion is input by user.

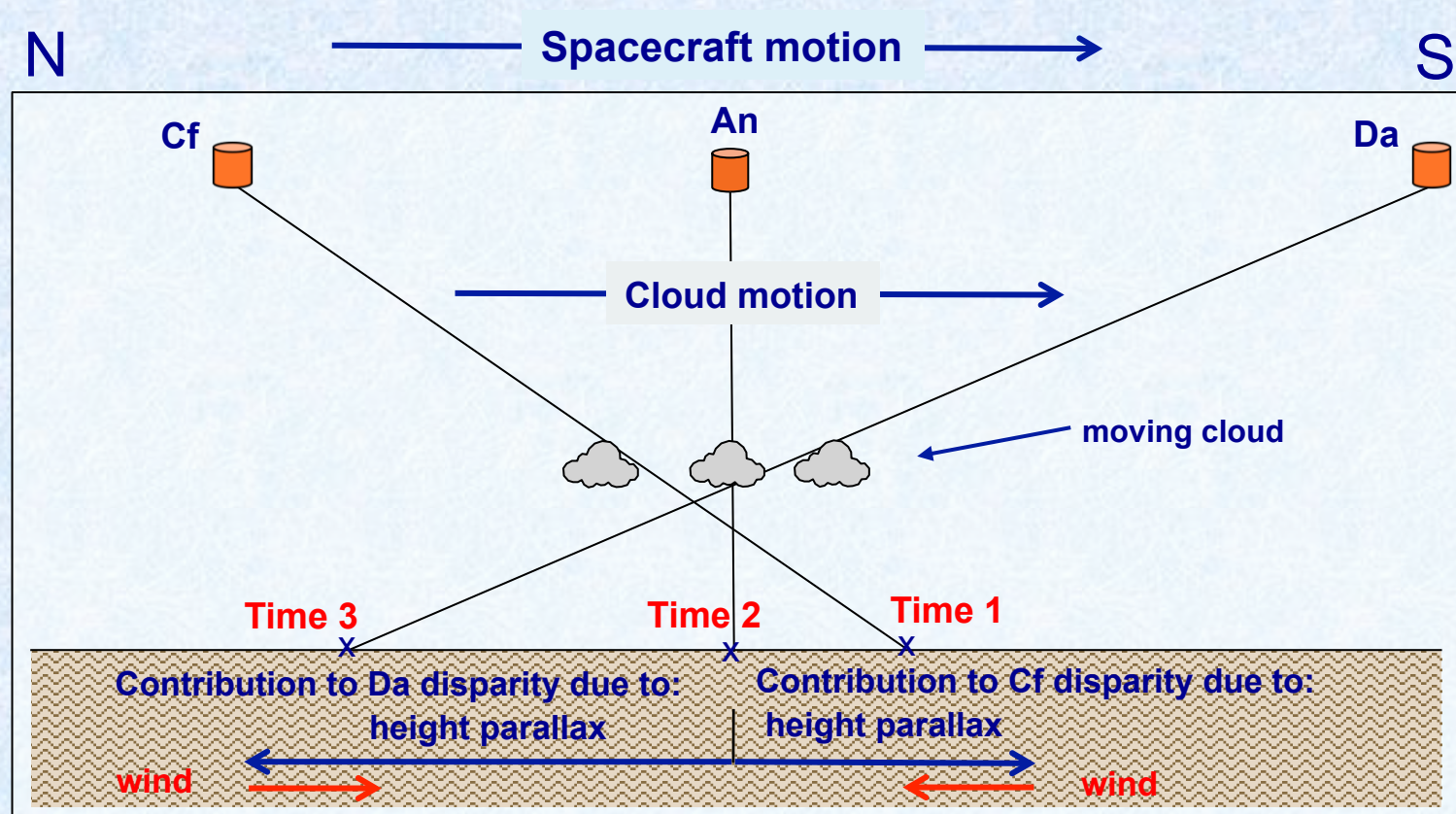


Cloud motion in direction opposite spacecraft motion

Disparity - 2

If entire disparity is attributed to height parallax (zero-wind height), then:

- For cloud and spacecraft motion in same direction, height estimate is too low
- For cloud and spacecraft motion in opposite directions, height estimate is too high



Cloud motion in same direction as spacecraft motion

Image Matching - 1

Objective: To find a feature in the image from a non-nadir camera that corresponds to a feature in the image from the An camera and to measure its disparity.

- In MINX, the **An** camera always acts as the reference image
- Six other cameras provide comparison images
- Image matching finds **disparities** between the target pixel location in reference image and the corresponding pixel location in the comparison image
- Disparity has SOM **across**-track and **along**-track components
- It can be applied to features **on** the earth's surface or **above** the surface
- MINX uses the correlation coefficient (**CC**) for assessing the quality of a match
- Image-matching will fail if the images lack texture or distinctive features

Reference image



Comparison image



Alaska fire with small pyrocumulus clouds showing effect of parallax (plus motion due to wind?)

Image Matching - 2

Correlation Coefficient:
$$r_{xy} = \frac{\sum (x_i - \bar{x})(y_i - \bar{y})}{(n-1)s_x s_y}$$

Where:

r_{xy} = correlation coefficient

x_i = BRF values at pixels in reference patch

\bar{x} = mean value of the BRFs in reference patch

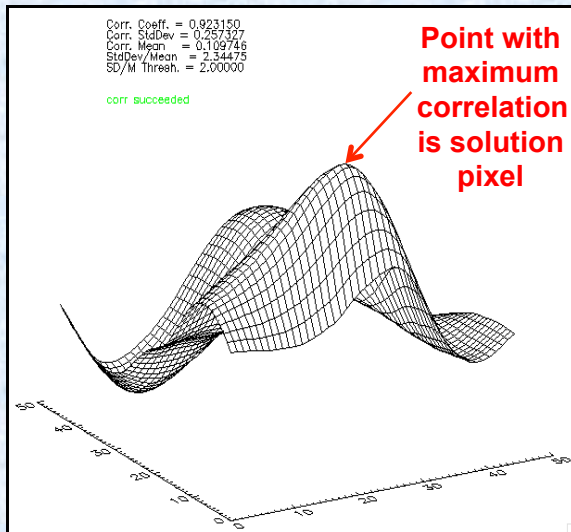
y_i = BRF values at pixels in comparison patch

\bar{y} = mean value of the BRFs in comparison patch

n = number of pixels in reference patch

s_x = standard dev. of BRF values in reference patch

s_y = standard dev. of BRF values in comparison patch



Correlation matrix interpolated to obtain sub-pixel resolution

Pass 2: An

Pass 2: Af
Before correlation
After correlation

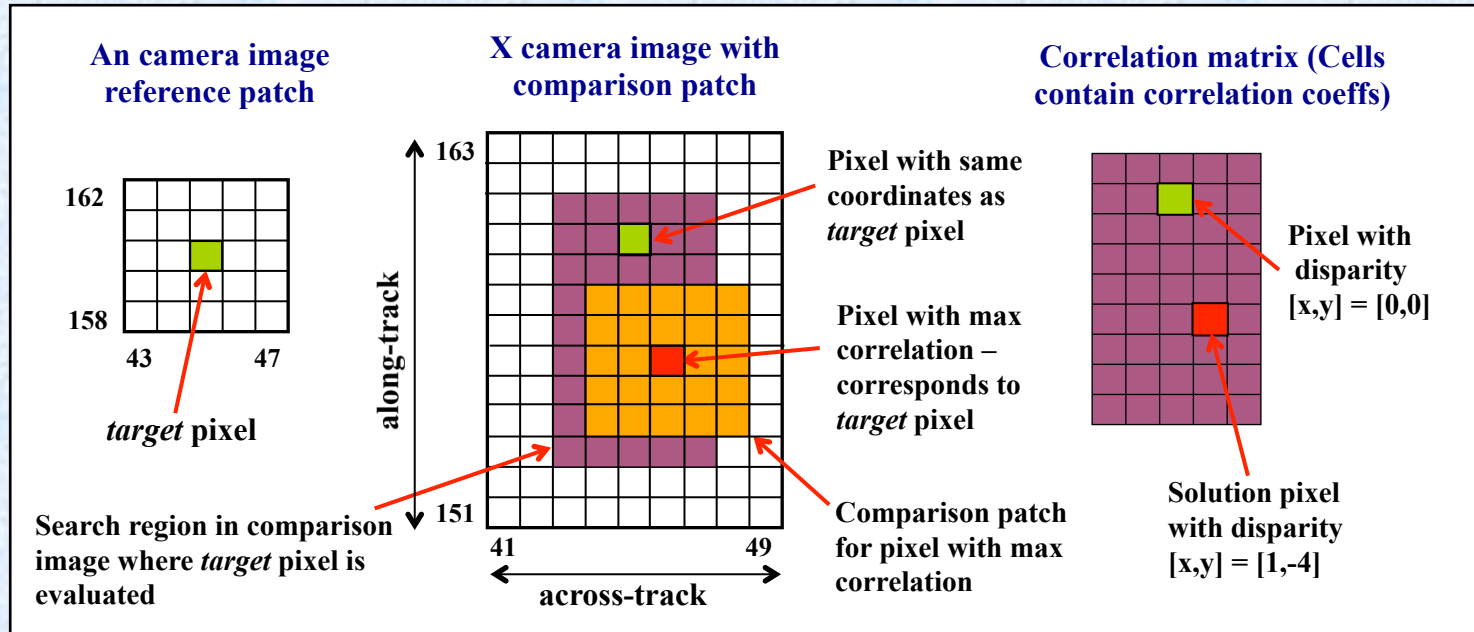
An red-band reference patch

Af red-band search region (red rectangle)

MINX reference patch from An image and search region from Af comparison image - the red + is the target pixel and the green x is solution pixel with highest correlation

- Correlation finds match to nearest pixel
- To increase precision, fit a bi-cubic surface to the correlation matrix around the solution pixel and interpolate to derive a finer grid
- Find the fine grid point with the largest **CC** - this gives fractional (sub-pixel) disparities

Image Matching - 3



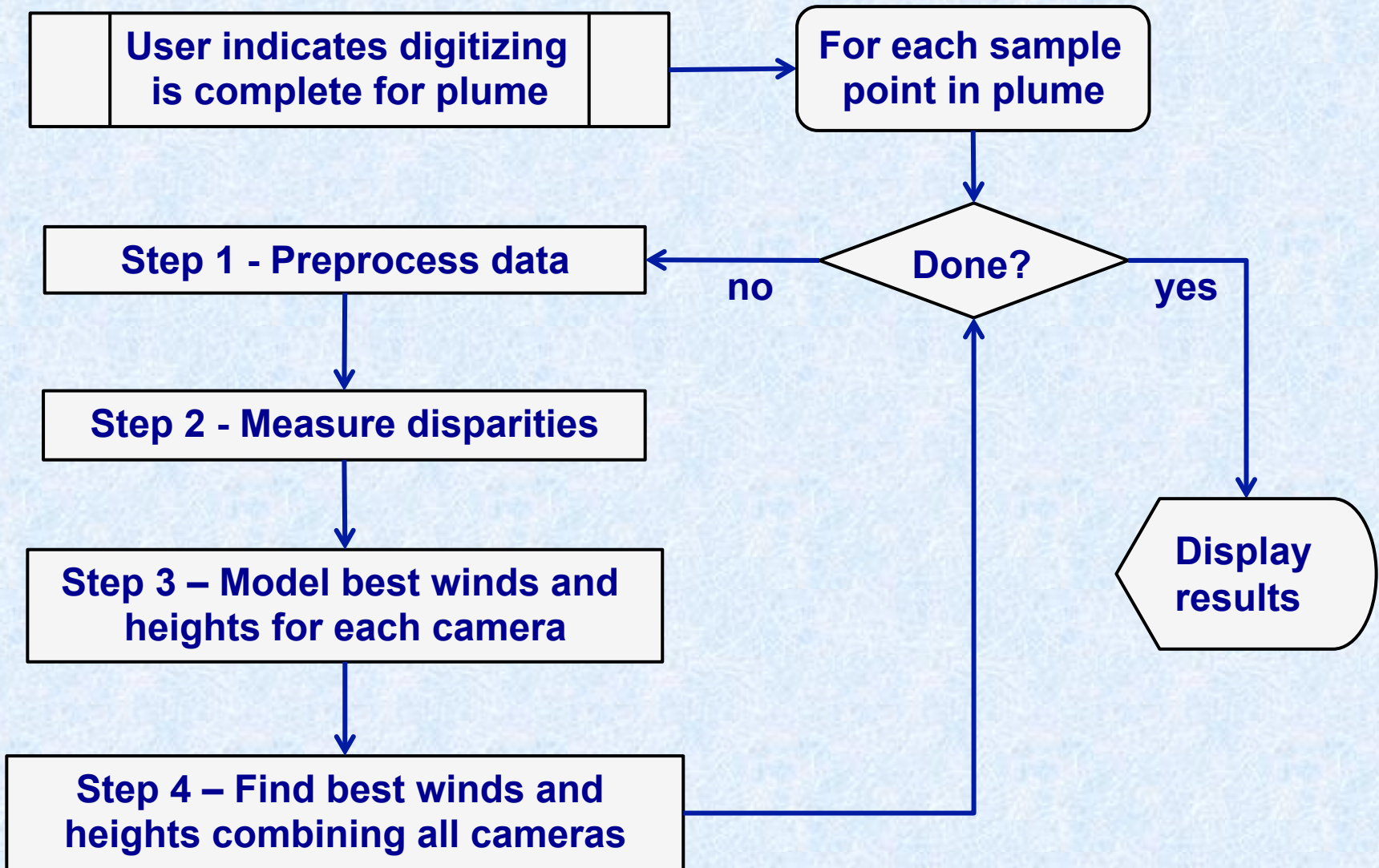
- ① Center the reference patch over the upper-left most pixel in the comparison image's search region
- ② Calculate correlation coefficient using BRFs for the overlapping pixels and place results into its corresponding location in correlation matrix
- ③ Slide the reference patch to next pixel in search region and compute CC again –repeat for all pixels in the search region
- ④ The pixel in the comparison image with highest CC is the match

Violet area is the search region where corresponding pixel is known to be based on computed maximum height and wind speed

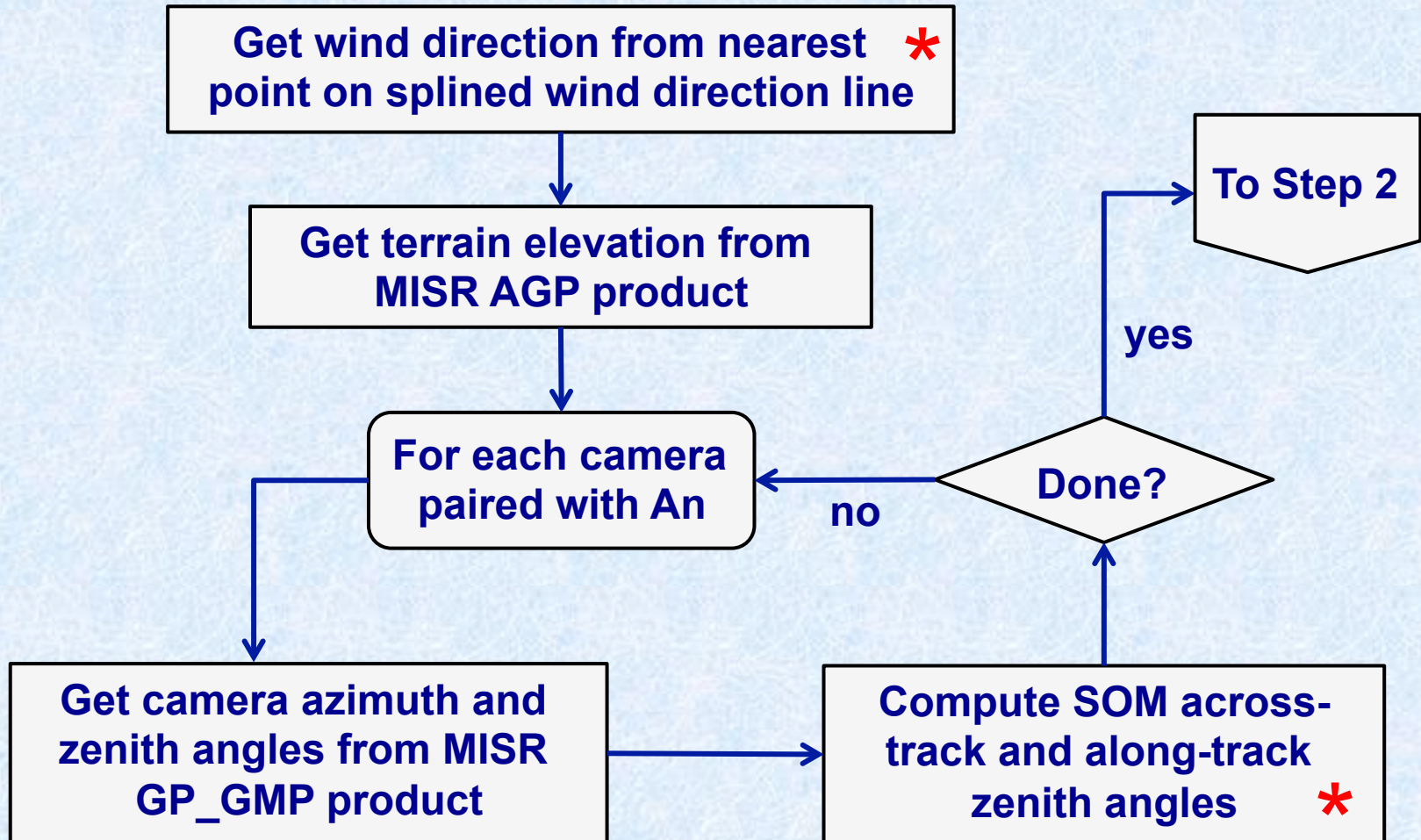
Contents

- **Parallax, disparity and image matching**
- **Height/wind retrieval algorithm**
- **MINX height retrieval comparisons**

MINX Top Level Algorithm

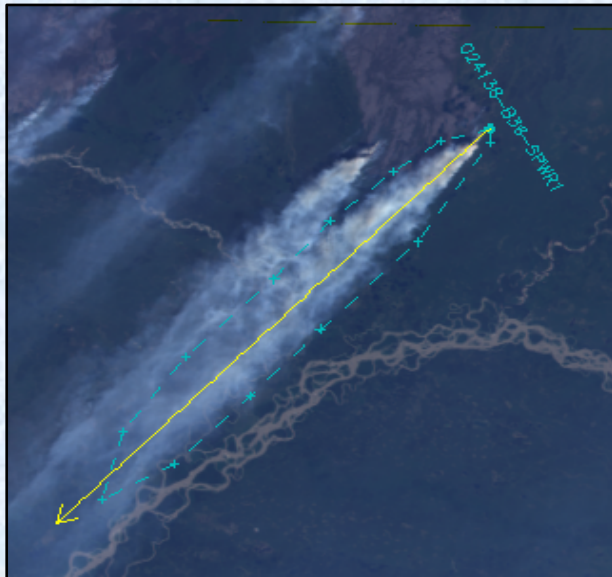


Step 1 - Preprocess Data

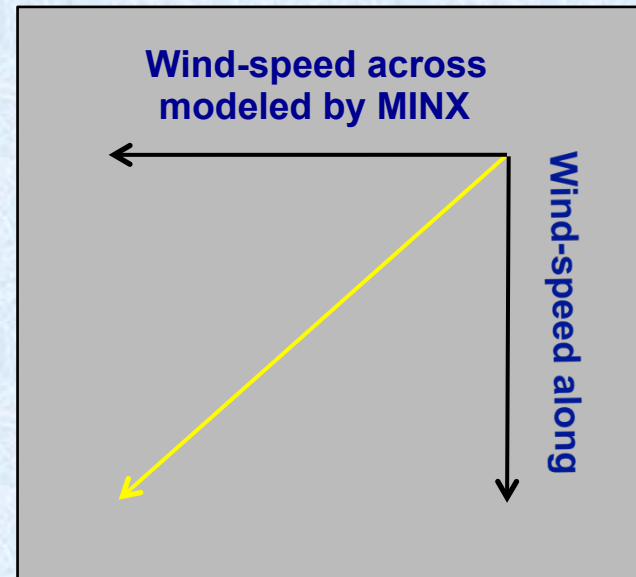


Get Wind Direction

- The height/wind retrieval problem has 3 unknowns :
 - height, wind-speed across-track and wind-speed along-track
- User inputs a (wind) direction of motion during digitizing
- If either the across-track or the along-track wind speed is known, the other component can be computed using the wind direction
- Thus the retrieval problem simplifies to 2 unknowns



Digitized plume showing
"wind direction" line in yellow



Wind-speed along-track is easily
computed from wind-speed
across-track plus wind direction

Compute Across and Along-Track Zenith Angles

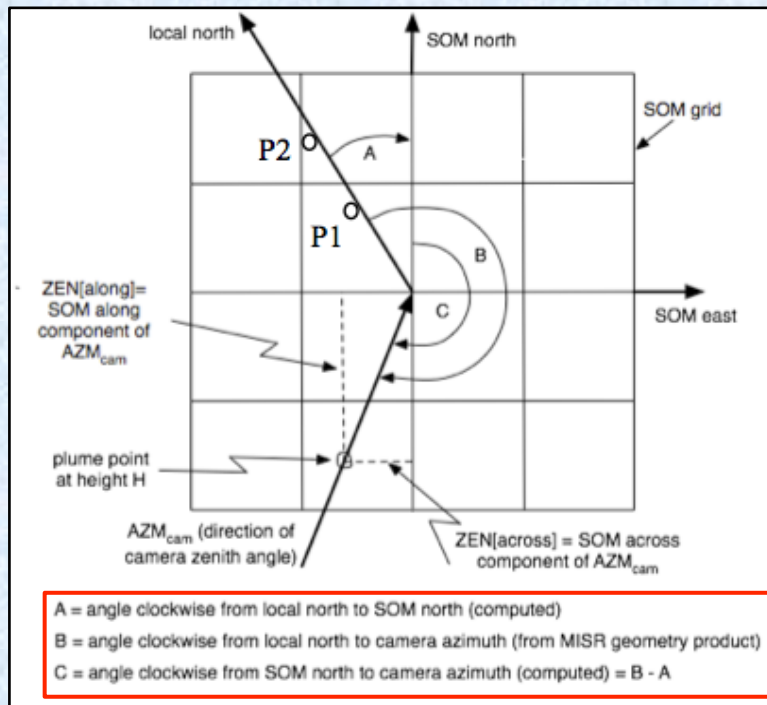
Objective: To convert camera azimuth angle and camera zenith angle into 2 orthogonal components of zenith angle in the SOM across-track and along-track directions. This allows us to compute the 2 components of disparity independently.

- ① Create a closely spaced pair of points $P1 = [lat1, long]$ and $P2 = [lat2, long]$ on the same geographic meridian in the region of interest, and project each to SOM coordinates
- ② Find distances (dx_{north}, dy_{north}) along the SOM_{north} and SOM_{east} axes between the points

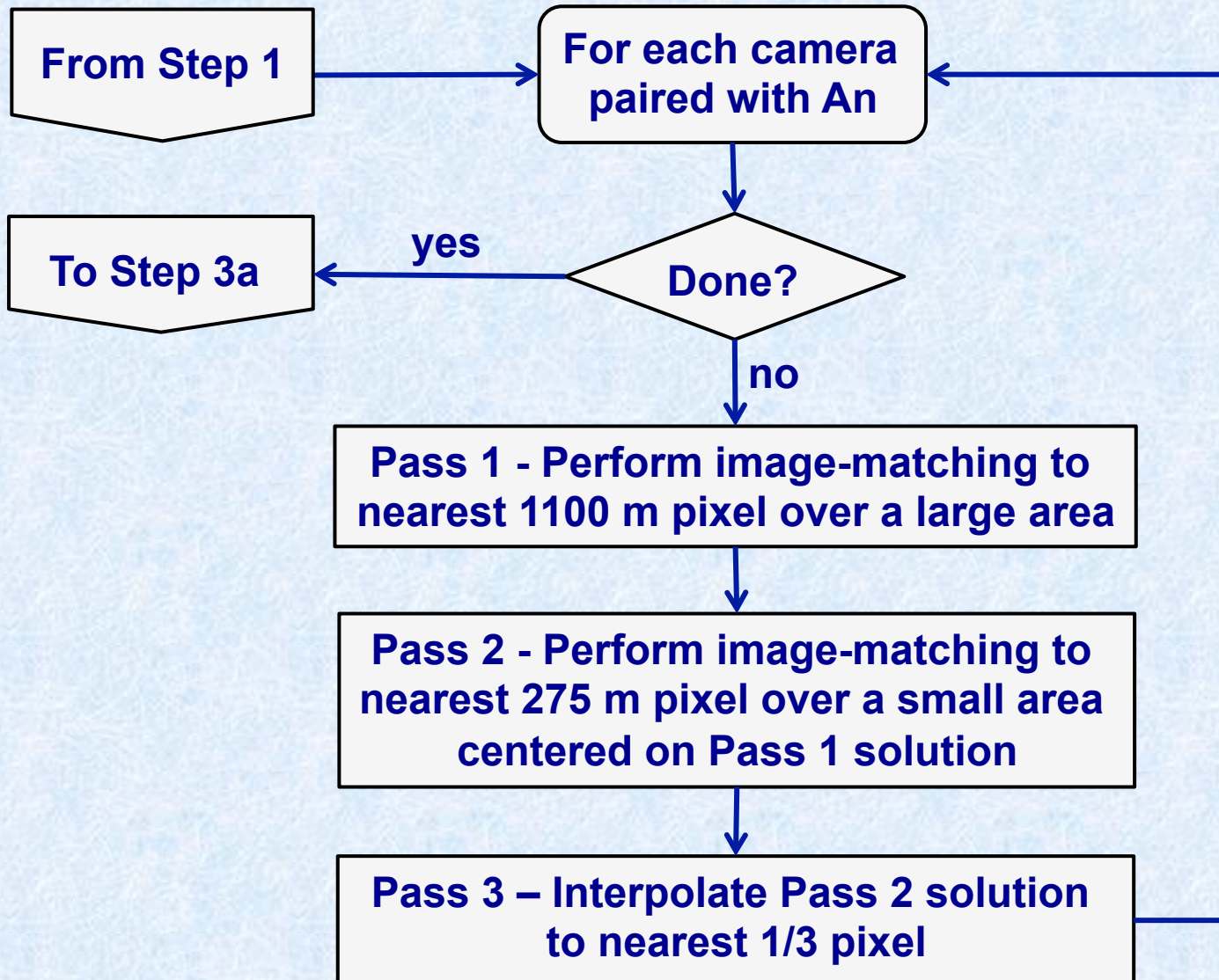
- ③ Compute the angle, A , clockwise from local north to SOM_{north} : $A = ATAN(dx_{north}, dy_{north})$
- ④ Compute the angle, C , clockwise from SOM_{north} to the azimuth direction of the camera (AZM_{cam}) to give the SOM-relative azimuth angle of the camera (AZM_{som}): $C = B - A$
- ⑤ Decompose the camera zenith angle (ZEN_{cam}) into across-track and along-track components to derive the SOM zenith angles (ZEN_{som}):

$$ZEN_{SOM}[\text{across}] = ZEN_{CAM} * SIN(AZM_{SOM})$$

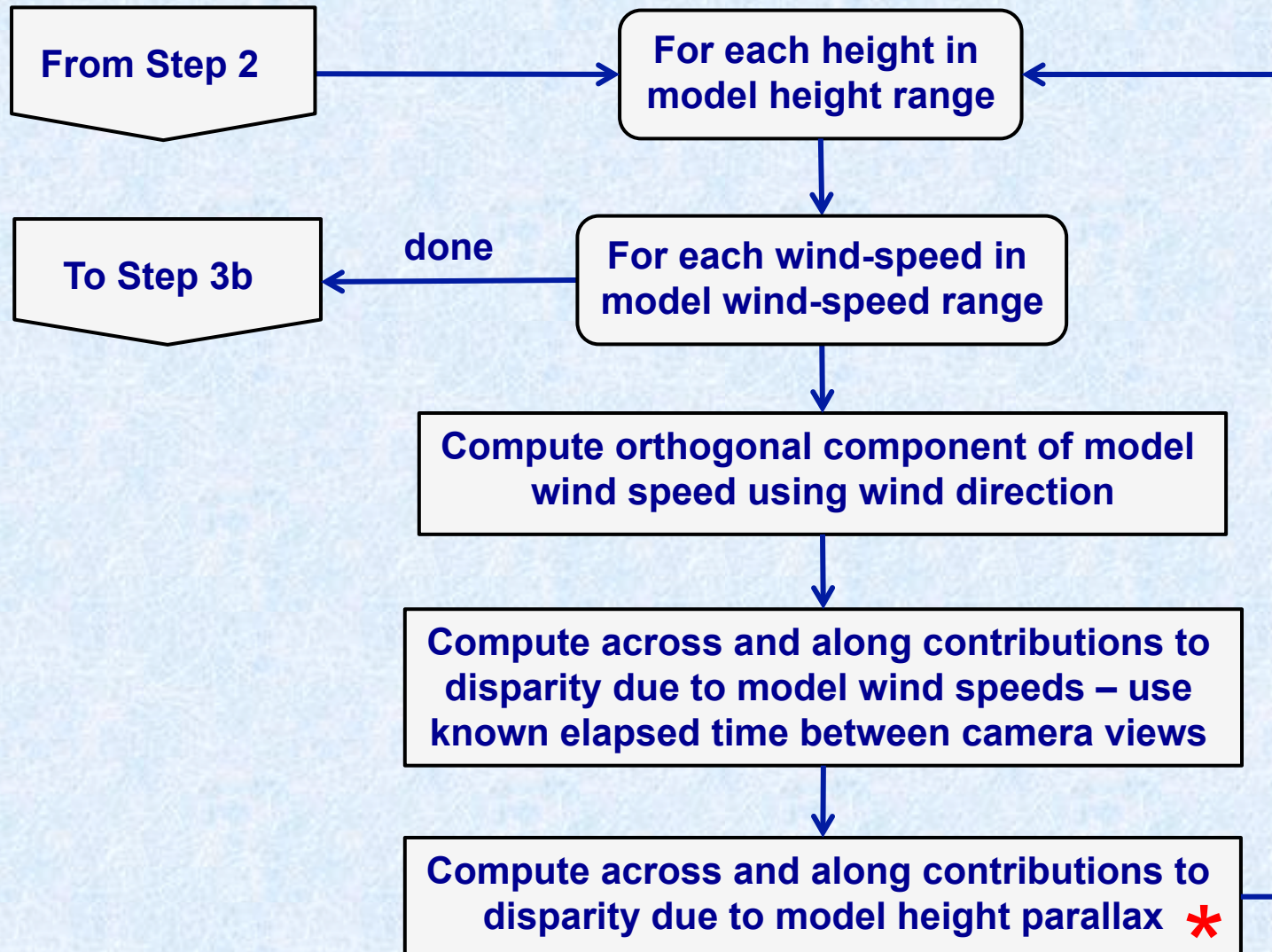
$$ZEN_{SOM}[\text{along}] = ZEN_{CAM} * COS(AZM_{SOM})$$



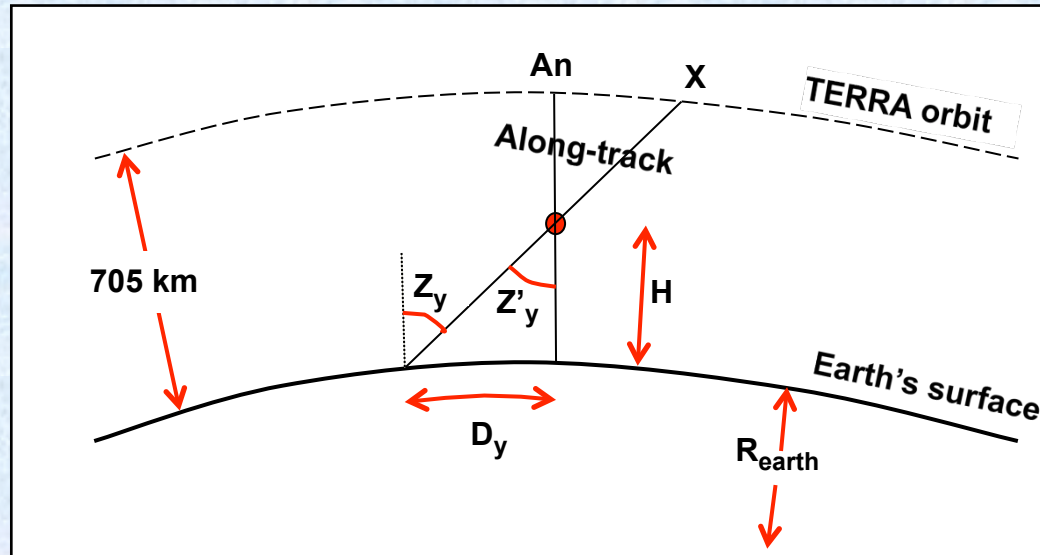
Step 2 – Measure Disparities



Step 3a – Forward Model Winds and Heights for Each Matched Camera



Compute Across and Along Contributions to Disparity due to Parallax



Earth geometry used in modeling along-track component of disparities due to height parallax

Forward modeling equation to compute disparity (D_y) for one camera in along-track direction:

$$D_y = \left(ASIN \left(\frac{H + R_{earth}}{R_{earth}} * SIN(Z'_y) \right) - Z'_y \right) * C_{earth}$$

The same equation is used to compute disparities in the across-track direction.

Where:

D_y = disparity in SOM y direction

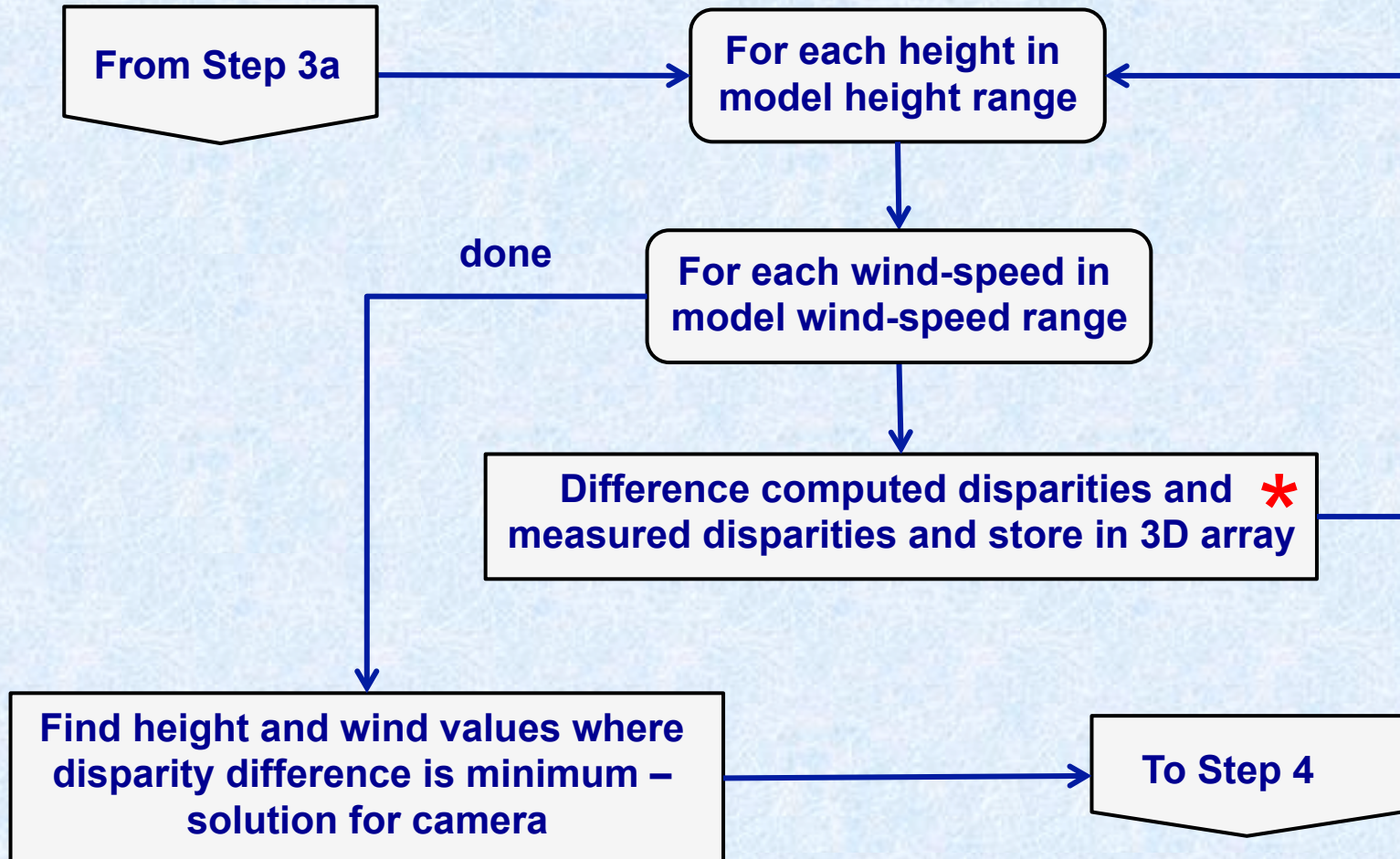
H = height of aerosol pixel above ellipsoid

R_{earth} = radius of earth = 6371 km

C_{earth} = circumference of earth = 40,030 km

Z'_y = zenith angle component in SOM_{along} direction (Z'_y closely approximates camera zenith angle Z_y)

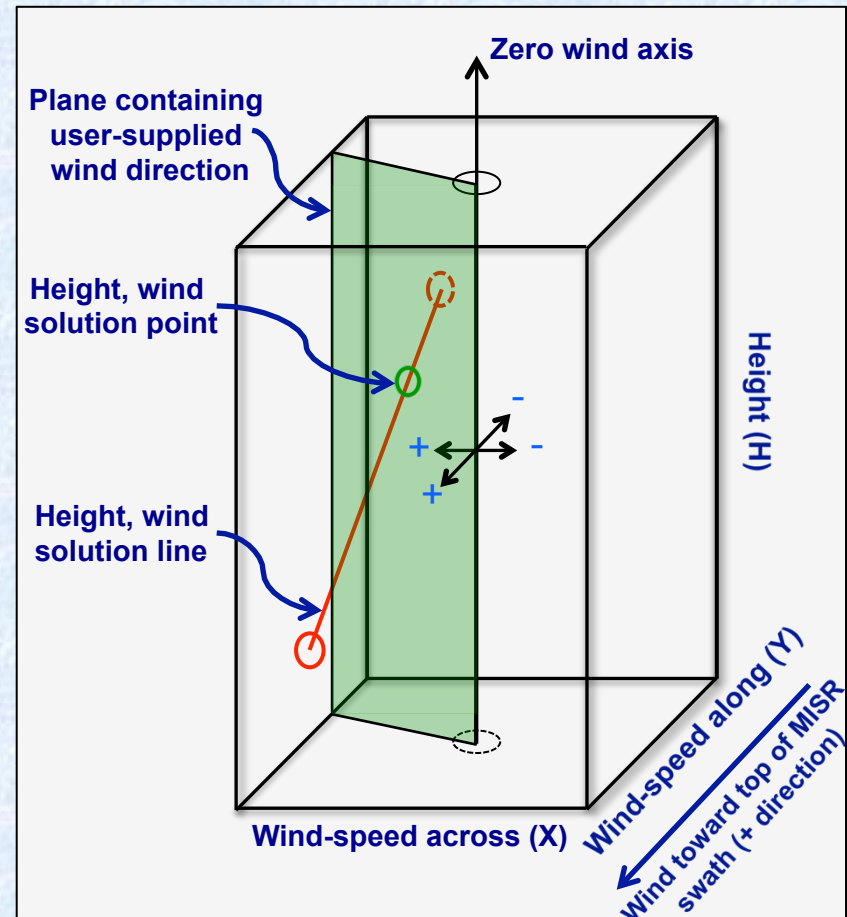
Step 3b – Find Best Height and Winds for Each Matched Camera



3D Data Cube of Disparity Differences

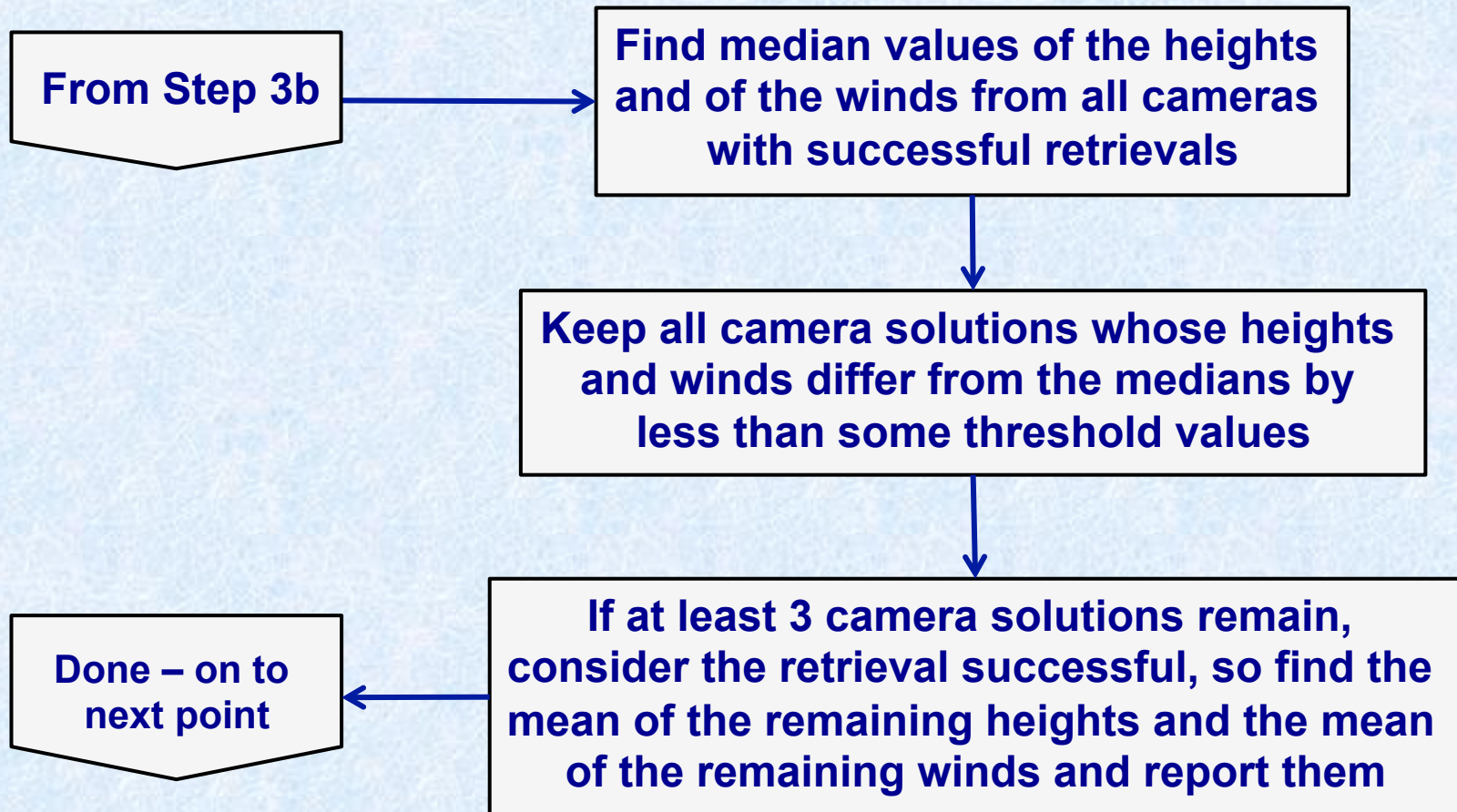
- Each node in the data array is indexed by model parameters X (wind-speed across), Y (wind-speed along) and H (height)
- Each node contains a disparity difference: $D_{\text{total}} = D_{\text{measured}} - D_{\text{modeled}}$
- Best height/wind solutions exist wherever $D_{\text{total}} = 0$; this is true for all points on a sloping line parallel to the wind-speed along axis
- The intersection of this line with a plane containing the user-supplied wind direction is the solution

If wind direction is known, modeling needs to be done only in the plane containing the wind direction - 3 unknowns reduce to 2 and a camera pair rather than a camera triplet is able to provide a unique solution



3D data array for solution of winds and height for one camera at one data point

Step 4 – Find Best Height and Winds Combining all Successful Cameras



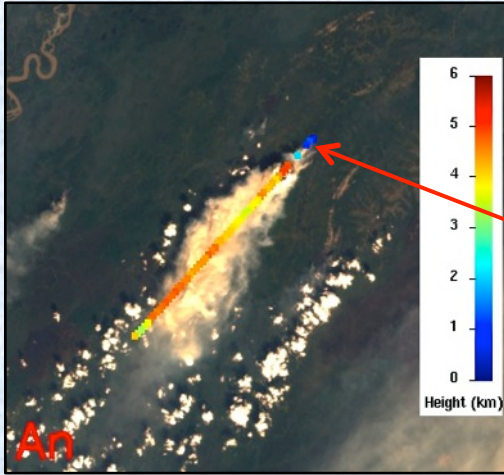
MISR vs. MINX Stereo Height Algorithms

Feature	MISR Standard Stereo Product	MINX
Level 1 imagery	Ellipsoid-projected	Terrain-projected
Matcher cost func	Mean of normalized differences	Pearson's correlation coefficient
Order of solution	Winds retrieved first, heights later	Winds and heights retrieved simultaneously
Cameras used	An / Bx / Dx triplets for wind Af / An / Aa triplets for height	Cf, Bf, Af, Aa, Ba, Ca, each paired with An for height and wind
Wind retrieval dependency	Depends on earth curvature viewed by D cameras and applicable to any feature above the terrain	Depends on knowledge of wind direction and generally applicable only to plumes or where wind direction is known
Wind resolution	Wind retrievals averaged over 70.4 km and applied to heights at 1.1 km	Heights and winds retrieved simultaneously at 1.1 km resolution
Number of unknowns	3: wind speed across-track, wind speed along-track and height	2: one wind speed plus height; the other wind speed is derived from user-supplied wind direction
Methodology	Finds unique inverse solution using 1 set of camera triplets (2 sets for wind)	Uses forward modeling that averages results of up to 8 camera pairs

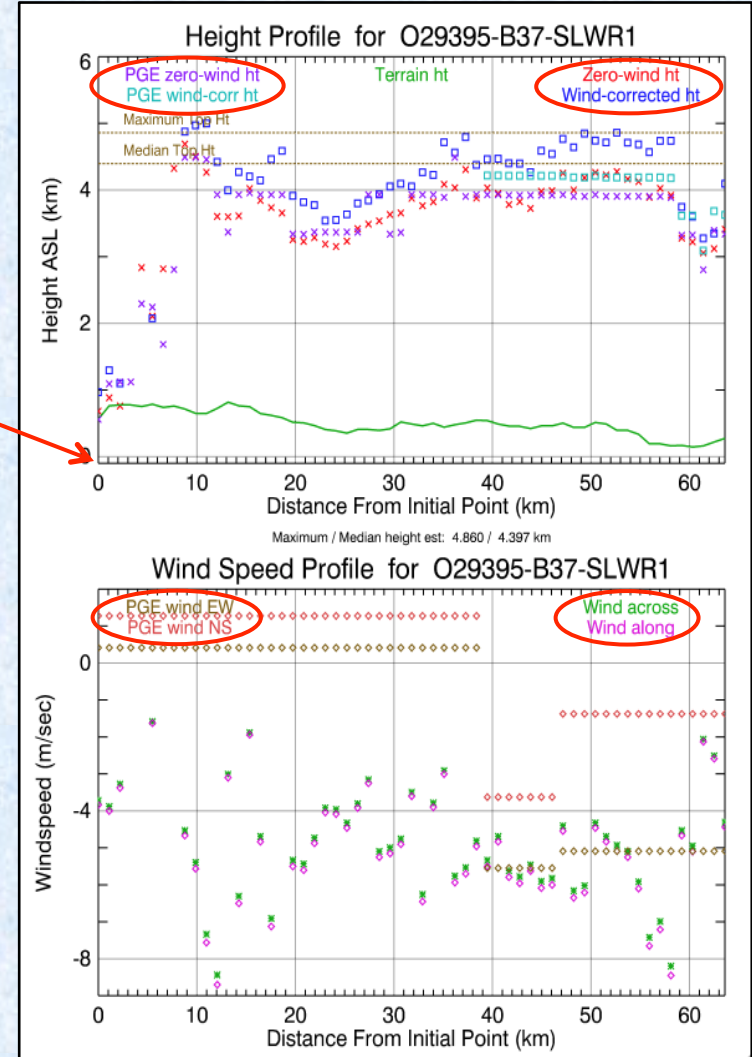
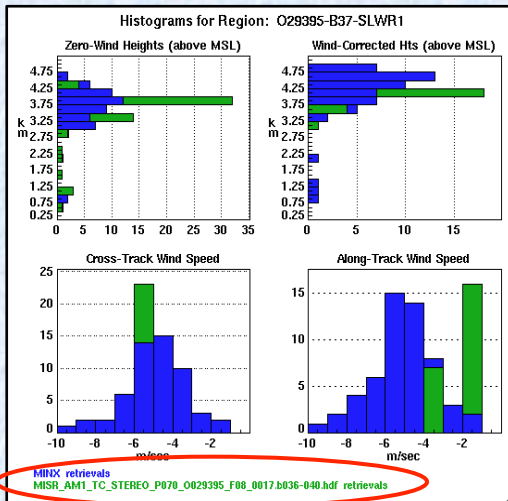
Contents

- **Parallax, disparity and image matching**
- **Height/wind retrieval algorithm**
- **MINX height retrieval comparisons**

MINX Height Retrieval Comparison - 1

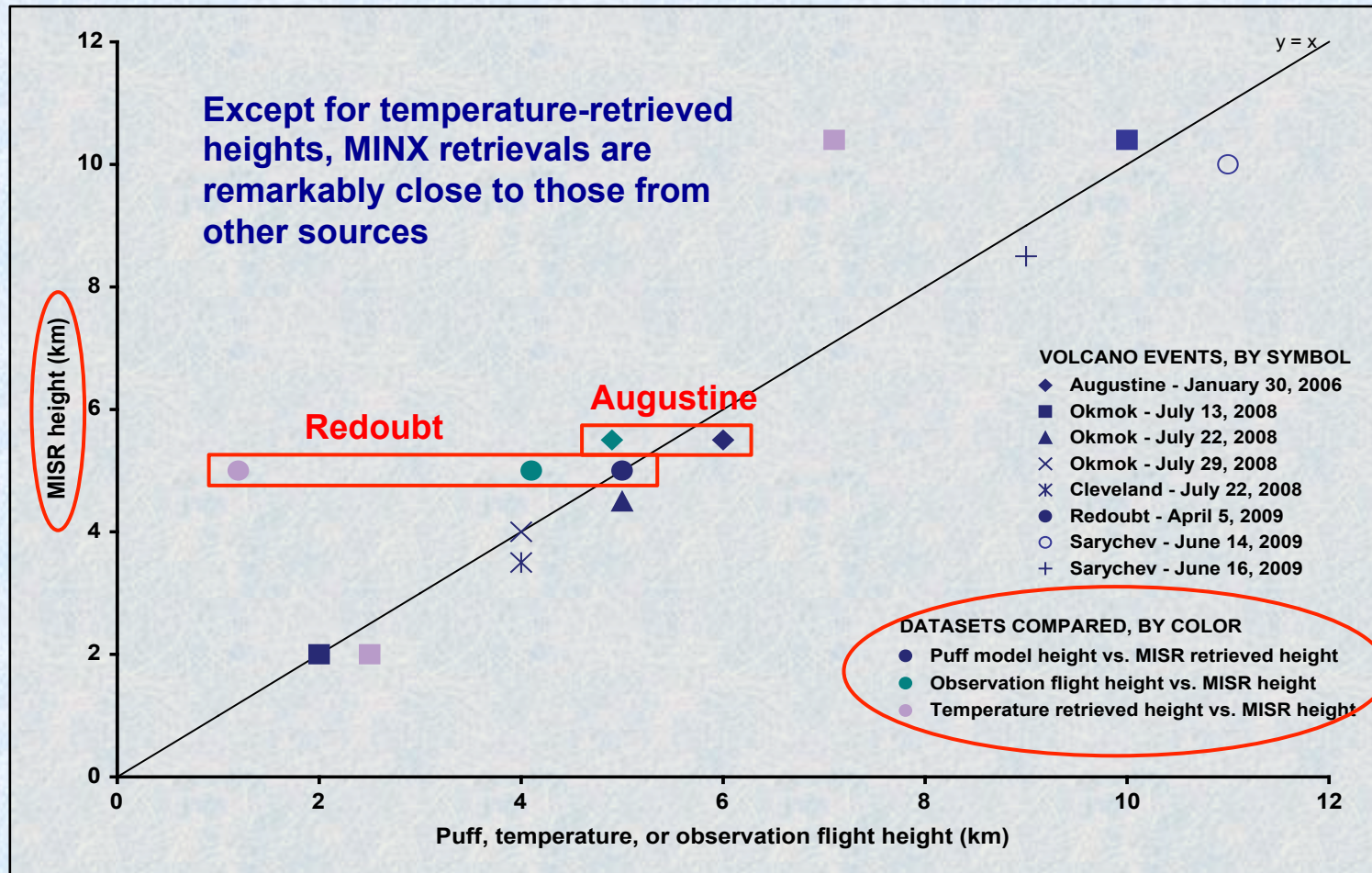


- MINX and MISR zero-wind and wind-corrected heights are similar
- MISR heights and winds are “quantized” due to matching at whole pixel level
- MISR winds are constant over large distances due to 70.4 km resolution retrieval
- Across-track winds are more similar than along-track winds
- A new version of the MISR stereo product produces significantly improved results



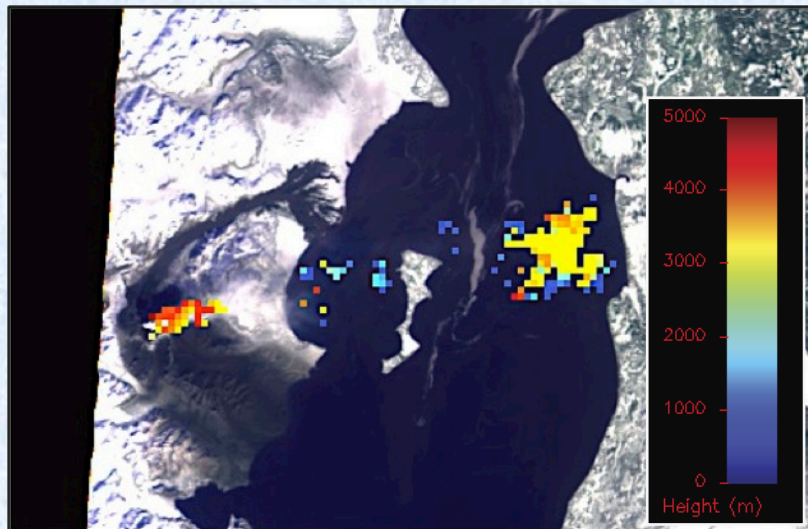
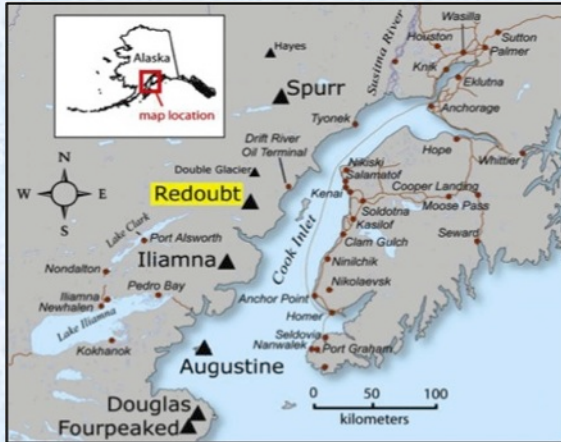
MINX Height Retrieval Comparison - 2

MINX plume heights for 8 Ring of Fire volcanic eruptions compared with heights from other sources

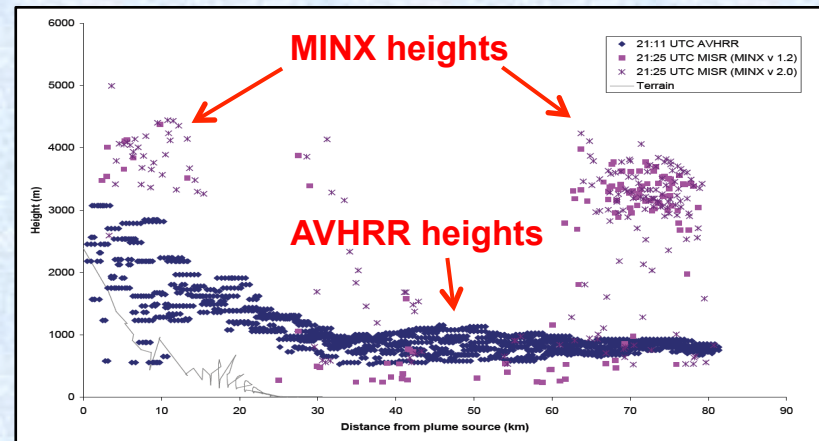


Courtesy of Angela Ekstrand, Alaska Volcano Observatory

Redoubt Eruption – Alaska – April 5, 2009



AVHRR retrieves heights near the water surface when the ash plume is thin

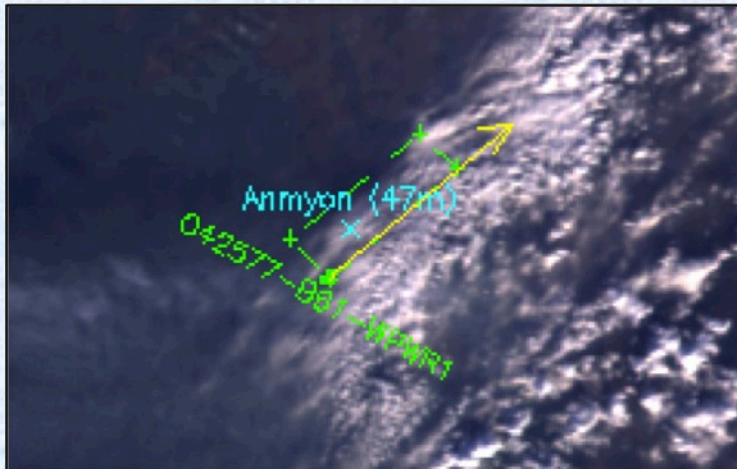


Images and analysis courtesy of Angela Ekstrand et al, AGU 2010

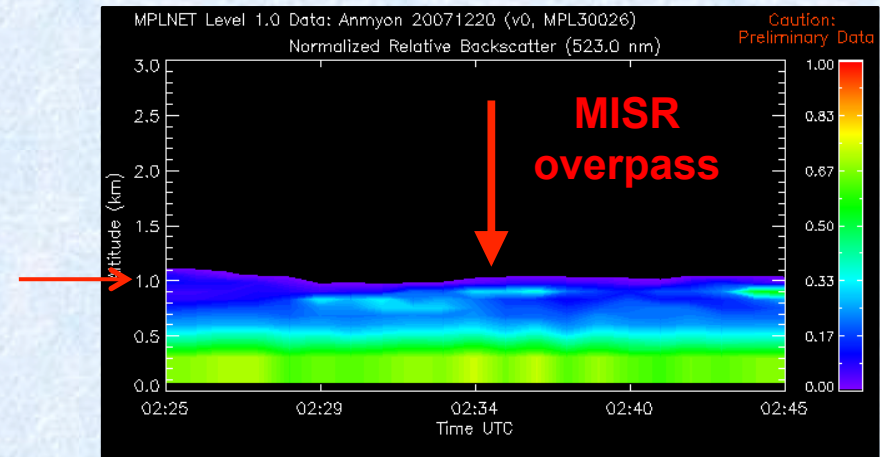
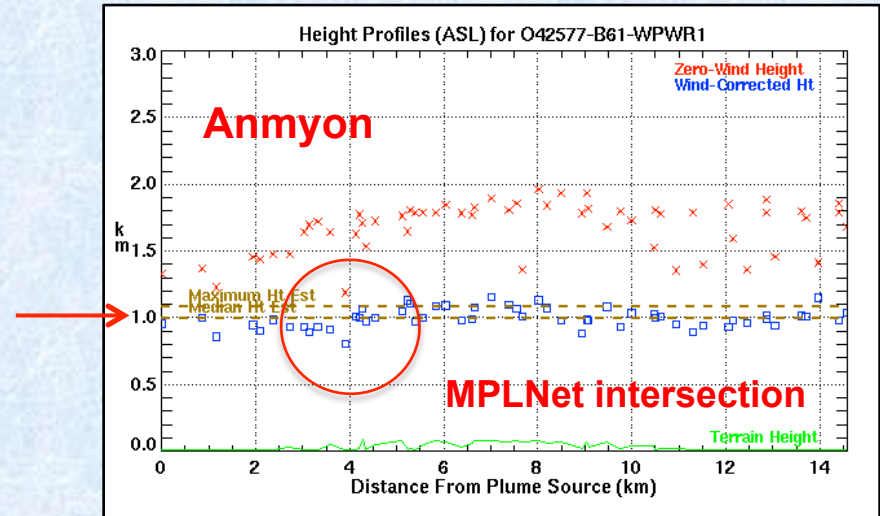
MINX Height Retrieval Comparison - 3

Collocation of micropulse lidar and MISR data at Anmyon on the coast of South Korea

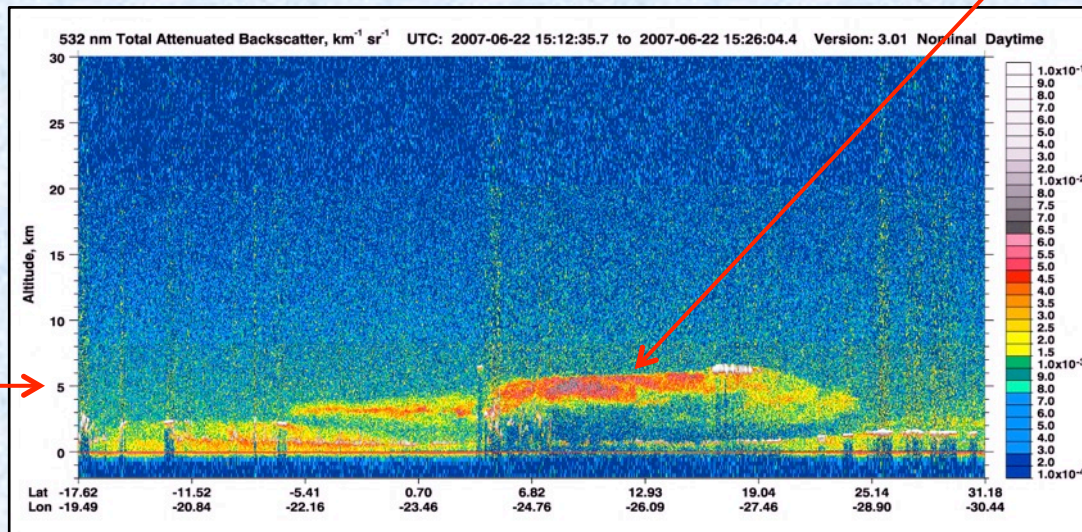
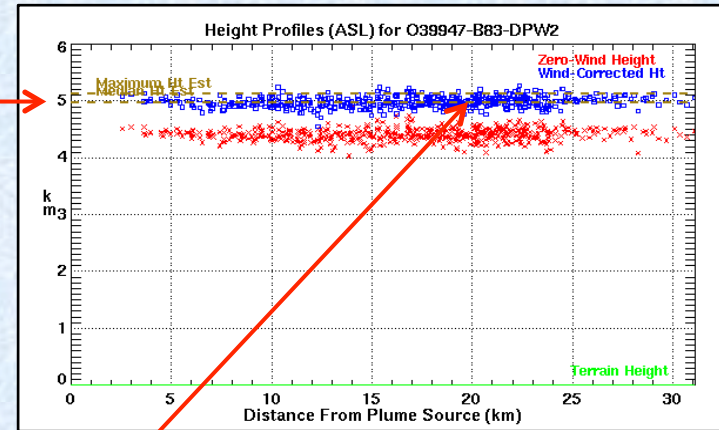
by Ben Dunst, UCLA
and Mike Garay, JPL



Wind direction for MINX retrieval derived from meteorological data



MINX Height Retrieval Comparison - 4



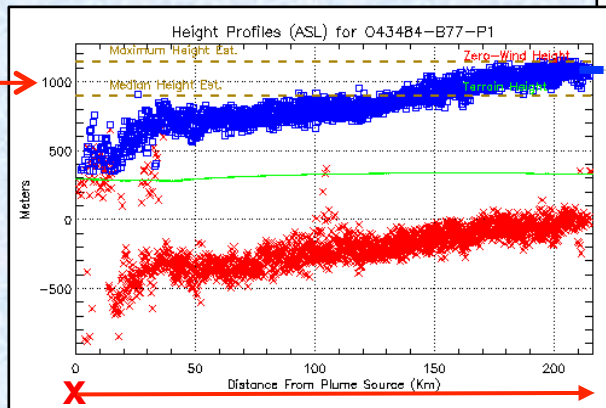
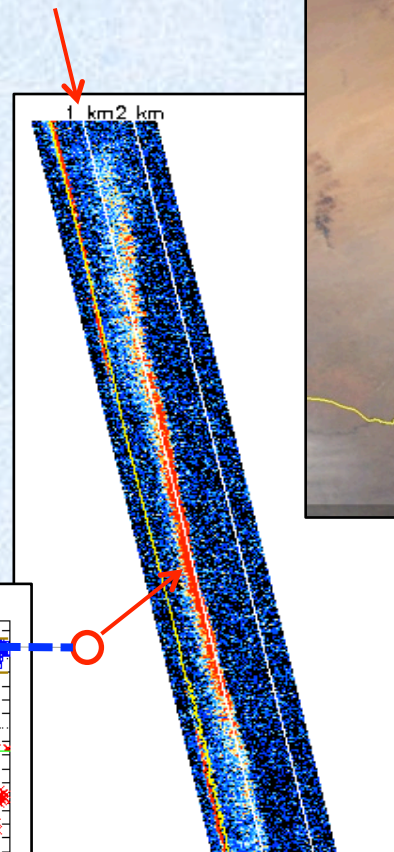
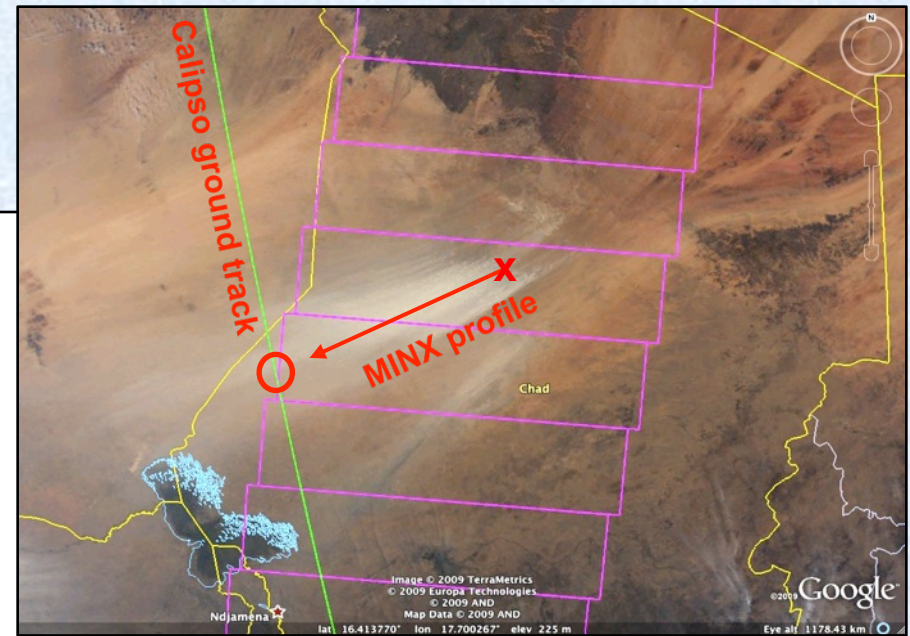
**Dust over Atlantic
Ocean off West Africa
seen by Calipso lidar
and MISR**

**by Olga Kalashnikova
and Mark Chodas, JPL**

MINX Height Retrieval Comparison - 5

Dust over Bodele Depression, Chad seen by Calipso lidar and MISR

by Mike Garay, JPL



References

- Chen, Y., Q. Li, J.T. Randerson, E.A. Lyons, R.A. Kahn, D.L. Nelson, and D.J. Diner, 2009. The sensitivity of CO and aerosol transport to the temporal and vertical distribution of North American boreal fire emissions, *Atm. Chem. Phys* 9, 6559-6580.
- Diner, D.J., D.L. Nelson, Y. Chen, R.A. Kahn, J. Logan, F-Y. Leung, and M. Val Martin, 2008. Quantitative studies of wildfire smoke injection heights with the Terra Multi-angle Imaging SpectroRadiometer. *SPIE Proceedings*.
- Kahn, R., Y. Chen, D.L. Nelson, F-Y. Leung, Q. Li, D.J. Diner, and J.A. Logan, 2008. Wildfire smoke injection heights – Two perspectives from space, *Geophys. Res. Lett.* 35, doi:10.1029/2007GL032165.
- Kahn, R. A., W.-H. Li, C. Moroney, D. J. Diner, J. V. Martonchik, and E. Fishbein (2007). Aerosol source plume physical characteristics from space-based multiangle imaging, *J. Geophys. Res.*, 112, D11205, doi:10.1029/2006JD007647.
- Mazzoni, D., J.A. Logan, D. Diner, R. Kahn, L. Tong, and Q. Li (2007). A data-mining approach to associating MISR smoke plume heights with MODIS fire measurements. *Rem. Sens. Environ.* 107, 138-148.
- Mims, S.R., R.A. Kahn, C.M. Moroney, B.J. Gaitley, D.L. Nelson, and M.J. Garay, 2009. MISR Stereo-heights of grassland fire smoke plumes in Australia. *IEEE Trans. Geosci. Remt. Sens.* 48, 25-35.
- Moroney, C., R. Davies, and J-P. Muller, 2002. MISR stereoscopic image matchers: Techniques and results, *IEEE Trans. Geosci. Remt. Sens.* 40, 1547-1559.
- Nelson, D. L., Y. Chen, R. A. Kahn, D. J. Diner, and D. Mazzoni, 2008. Example applications of the MISR Interactive eXplorer (MINX) software tool to wildfire smoke plume analyses. *Proceedings of SPIE*, 7089, 708909.1-708909.11.
- Sofiev, M., T. Ermakova, and R. Vankevich, 2012. Evaluation of the smoke-injection height from wild-land fires using remote-sensing data, *Atmos. Chem. Phys.*, 12, 1995–2006, doi:10.5194/acp-12-1995-2012.
- Tosca, M.G., J.T. Randerson, C.S. Zender, D.L. Nelson, D.J. Diner, and J.A. Logan, 2011. Dynamics of fire plumes and smoke clouds associated with peat and deforestation fires in Indonesia, *J. Geophys. Res.*, VOL. 116, D08207, 14 pp, doi: 10.1029/2010JD015148.
- Val Martin, M., J.A. Logan, R. Kahn, F-Y. Leung, D. Nelson, and D. Diner, 2010. Smoke injection heights from fires in North America: Analysis of five years of satellite observations, *Atm. Chem. Phys.* 10, 1491-1510.
- Wu, D.L., Diner, D.J., Garay, M.J., Jovanovic, V.M., Lee, J.N., Moroney, C.M., Mueller, K.J., and Nelson, D.L., 2010. MISR CMVs and Multiangular Views of Tropical Cyclone Inner-Core Dynamics, *Proceeding of IWW10*.
- Zong, J., R. Davies, J.P. Muller, and D.J. Diner, 2002. Photogrammetric retrieval of cloud advection and top height from the multi-angle imaging spectroradiometer (MISR). *Journal of the American Society for Photogrammetric Engineering and Remote Sensing*, 68 (8), 821-830.